# Reduced-order model for nonlinear dynamical structures having numerous local elastic modes in the low-frequency range

Anas Batou, Christian Soize, N. Brie

# Reduced-order model for nonlinear dynamical structures having numerous local elastic modes in the low-frequency range.

**A. Batou** [1] **, C. Soize** [1] **, N. Brie** [2]

[1] Université Paris-Est, Laboratoire Modélisation et Simulation Multi Echelle,
MSME UMR 8208 CNRS, 5 bd Descartes, 77454 Marne-la-Vallee, France
e-mail: **anas.batou@univ-paris-est.fr**

[2] EDF R&D, Département AMA, 1 avenue du général De Gaulle, 92140 Clamart, France

## Abstract

This research is devoted to the construction of a reduced-order computational model for nonlinear dynamical structures which are characterized by the presence of numerous local elastic modes in the low-frequency band. Therefore these structures have a high modal density in the low-frequency band and the use of the classical modal analysis method is not suited here. We propose to construct a reduced-order computational model using a small-dimension basis of a space of global displacements, which is constructed *a priori* by solving an unusual eigenvalue problem. Then the reduced-order computational model allows the nonlinear dynamical response to be predicted with a good accuracy on the stiff part of the structure. The methodology is applied to a complex industrial structure which is made up of a row of seven fuel assemblies with possibility of collisions between grids and which is submitted to a seismic loading.

## 1 Introduction

This paper is devoted to the construction of a reduced-order model for nonlinear dynamical structures having numerous local elastic modes in the low-frequency (LF) range. This paper focuses specifically on localized non-linearities such as elastic stops. We are interested in the nonlinear response of structures which are made up of a rigid master structure (the stiff part) coupled with several flexible substructures. Such structures are characterized by the fact that they present in the LF band, both classical global elastic modes but also many local elastic modes. Moreover, the structure we consider is modeled with a large finite element model and has several localized nonlinearities (such as elastic stops). As a consequence, the non-linear transient response has to be constructed using a small time step for the integration scheme in order to correctly capture the nonlinear effects in the non-linear transient response. Then, the direct construction of the non-linear transient response is a very challenging issue and therefore the computational model has to be reduced. Due to the high modal density of the structures under consideration, the classical reduction consisting in using the elastic modes of the underlying linear part of the nonlinear dynamical system is not suited here. Since we want to construct a small-dimension reduced-order computational model which has the capability to predict the nonlinear dynamical responses on the stiff part for which the local displacements are negligible, we have to construct the reduced-order computational model using a basis adapted to the prediction of the global displacements and therefore, we have to filter the local displacements in the construction of the basis. To achieve this objective, most of previous researches have been based on a spatial filtering of the short wavelengths. Concerning numerical methods, most of the techniques are based on the lumped mass methods. In the Guyan method [5], the masses are lumped at few nodes and the inertia forces of the other nodes are neglected. It should be noted that the choice of concentration points is not obvious to perform for complex

structures. The convergence properties of the solution obtained using the lumped mass method have been studied [3, 7, 2]. In [10], the authors propose to construct a basis of the global displacements space using a rough finite element model. For slender dynamical structures, another method consists in the construction of an equivalent beam or plate model [12, 13]. The Proper Orthogonal Decomposition (POD) method (see [9, 11]) allows in some cases to extract an accurate small size basis in order to construct a reduced-order computational model of a nonlinear dynamical system, but this basis has to be constructed *a posteriori*, which means that a sufficiently rich nonlinear response has to be constructed. Moreover, the POD basis is only optimal for a given external load (or imposed displacement).

Recently, a new method has been proposed to construct a reduced-order computational model in linear structural dynamics for structures having numerous local elastic modes in the low-frequency band [14]. In this method, a basis of the global displacements space and a basis of the local displacements space are calculated by solving two unusual eigenvalues problems. The elements of these two bases are not constituted of the usual elastic modes. The eigenvalue problem, allowing a basis of the global displacements space to be constructed, is constructed by introducing a kinematic reduction for the kinetic energy while the elastic energy is kept exact. In this paper, this method will be used to construct a basis of the global displacements space and then to deduce the reduced-order computational model of the nonlinear dynamical structure. Therefore, the contributions of the local displacements of the structure observed on the stiff part are neglected in the research presented here.

In Section 2, the method developed in [14] is summarized and the construction of the reduced-order computational model is presented. In Section 3, an industrial application is given. This application concerns the nonlinear transient response of a row of fuel assemblies.

## 2   Construction of the reduced-order computational model

In this Section, we first summarize the method introduced in [14] which allows a reduced-order computational model to be constructed for structures having a high modal density in the low-frequency range. Although this method allows both a basis of the global displacements space and a basis of the local displacements space to be constructed, we will only summarize the construction of the basis of the global displacements space (as previously explained, the contributions of the local displacements of the structure observed on the stiff part are neglected).

### 2.1   Reference non-linear computational model

We are interested in predicting the transient responses of a three-dimensional nonlinear damped structure, with localized nonlinearities, and occupying a bounded domain $\Omega$. The real-valued vector $\mathbb{U}(t)$ of the $m$ degrees of freedom (DOFs) of the computational model constructed with the finite element method, is solution of the following matrix equation,

$$[\mathbb{M}]\ddot{\mathbb{U}}(t) + [\mathbb{D}]\dot{\mathbb{U}}(t) + [\mathbb{K}]\mathbb{U}(t) + \mathbb{F}^{\text{NL}}(\mathbb{U}(t), \dot{\mathbb{U}}(t)) = \mathbb{F}(t) \quad , t \in ]0, T], \tag{1}$$

with the initial conditions

$$\mathbb{U}(0) = \dot{\mathbb{U}}(0) = \mathbf{0} \quad , \tag{2}$$

in which $[\mathbb{M}]$, $[\mathbb{D}]$ and $[\mathbb{K}]$ are respectively the $(m \times m)$ positive-definite symmetric real mass, damping and stiffness matrices, where $\mathbb{F}^{\text{NL}}(\mathbb{U}(t), \dot{\mathbb{U}}(t))$ is the vector of the nonlinear forces induced by the localized nonlinearities and where $\mathbb{F}(t)$ is relative to the discretization of the external forces. Usually, the nonlinear matrix equation (1) is reduced using the elastic modes of the linear part of Eq. (1). These modes are therefore such that $([\mathbb{K}] - \lambda[\mathbb{M}])\varphi = \mathbf{0}$. Since it is assumed that there are numerous local elastic modes and since there are nonlinear forces, one would need to calculate a high number of elastic modes in order to obtain a good convergence for the nonlinear dynamical response in the low-frequency range. The use of a basis of the global displacements space circumvents this difficulty.

## 2.2 Kinematic reduction of the kinetic energy

The methodology proposed in [14] consists in introducing a kinematic reduction of the structural kinetic energy. In a first step, the domain $\Omega$ is partitioned into $n_J$ disjoint subdomains $\Omega_j$. In a second step, this decomposition is used to construct the projection linear operator $\boldsymbol{u} \mapsto h^r(\boldsymbol{u})$ such that $h^r(h^r(\boldsymbol{u})) = h^r(\boldsymbol{u})$ and defined by

$$\{h^r(\boldsymbol{u})\}(\boldsymbol{x}) = \sum_{j=1}^{n_J} \mathbb{1}_{\Omega_j}(\boldsymbol{x}) \frac{1}{m_j} \int_{\Omega_j} \rho(\boldsymbol{x}') \, \boldsymbol{u}(\boldsymbol{x}') \, d\boldsymbol{x}' \, , \tag{3}$$

in which $\boldsymbol{x} \mapsto \mathbb{1}_{\Omega_j}(\boldsymbol{x}) = 1$ if $\boldsymbol{x}$ is in $\Omega_j$ and $= 0$ otherwise, where $m_j$ is the total mass of subdomain $\Omega_j$ and where $\rho(\boldsymbol{x})$ is the mass density. This operator carries out an average of the displacements with respect to the mass density in each subdomain (kinematic reduction). We then introduce the $(m \times m)$ matrix $[H^r]$ relative to the finite element discretization of the projection operator $h^r$ defined by Eq. (3), such as $[H^r]^2 = [H^r]$. Then, the $(m \times m)$ projected mass matrix $[\mathbb{M}^r]$ is constructed such that $[\mathbb{M}^r] = [H^r]^T[\mathbb{M}][H^r]$ with the following property

$$[\mathbb{M}^r] = [\mathbb{M}][H^r] = [H^r]^T[\mathbb{M}] \quad . \tag{4}$$

The rank of mass matrix $[\mathbb{M}^r]$ is $3\,n_J$.

## 2.3 Basis of the global displacements space.

The basis of the global displacements space is made up of the solutions $\boldsymbol{\varphi}^g$ in $\mathbb{R}^m$ of the generalized eigenvalue problem

$$[\mathbb{K}]\boldsymbol{\varphi}^g = \lambda^g[\mathbb{M}^r]\boldsymbol{\varphi}^g \, , \tag{5}$$

in which the stiffness matrix is kept exact while the mass matrix is projected. This generalized eigenvalue problem admits an increasing sequence of $3\,n_J$ positive global eigenvalues $0 < \lambda_1^g \le \ldots \le \lambda_{3n_J}^g$, associated with the finite family of algebraically independent eigenvectors $\{\boldsymbol{\varphi}_1^g, \ldots, \boldsymbol{\varphi}_{3n_J}^g\}$. The family $\{\boldsymbol{\varphi}_1^g, \ldots, \boldsymbol{\varphi}_{3n_J}^g\}$ spans a subspace of dimension $3\,n_J$ defined as the global displacements space. In general, this family is not made up of elastic modes. The computation of the eigenvectors is carried out using an adapted subspace iteration algorithm. This algorithm avoid the assembly of matrix $[\mathbb{M}^r]$ which is a full matrix. If needed, a basis of the local displacements space can also be constructed and complete the basis of global displacements (see [14]).

## 2.4 Reduced-order computational model

The reduced-order computational model is obtained using the projection of $\mathbb{U}(t)$ on the subspace of $\mathbb{R}^m$ spanned by the family $\{\boldsymbol{\varphi}_1^g, \ldots, \boldsymbol{\varphi}_{n_g}^g\}$ of real vectors associated with the $n_g$ first eigenvalues $0 < \lambda_1^g \le \ldots \le \lambda_{n_g}^g$, such that $n_g \le 3\,n_J \le m$. Let $[\Phi^g] = [\boldsymbol{\varphi}_1^g \ldots \boldsymbol{\varphi}_{n_g}^g]$ be the $(m \times n_g)$ real matrix whose columns are the vectors $\boldsymbol{\varphi}_1^g, \ldots, \boldsymbol{\varphi}_{n_g}^g$. Then, the $n_g$-order approximation $\mathbb{U}_{n_g}(t)$ of $\mathbb{U}(t)$ is written as

$$\mathbb{U}_{n_g}(t) = \sum_{j=1}^{n_g} \boldsymbol{\varphi}_j^g q_j{}^g(t) = [\Phi^g]\boldsymbol{q}^g(t) \quad , \tag{6}$$

in which $\boldsymbol{q}^g(t) = (q_1^g(t), \ldots, q_{n_g}^g(t))$. The vector $\boldsymbol{q}^g(t)$ is solution of the following nonlinear reduced matrix equation

$$[M]\ddot{\boldsymbol{q}}^g(t) + [D]\dot{\boldsymbol{q}}^g(t) + [K]\boldsymbol{q}^g(t) + \boldsymbol{f}^{\mathrm{NL}}(\boldsymbol{q}^g(t), \dot{\boldsymbol{q}}^g(t)) = \boldsymbol{f}(t) \quad , t \in ]0\,, T]\,, \tag{7}$$

with the initial conditions

$$\boldsymbol{q}^g(0) = \dot{\boldsymbol{q}}^g(0) = \boldsymbol{0} \quad , \tag{8}$$

in which $[M]$, $[D]$ and $[K]$ are the $(n_g \times n_g)$ generalized mass, damping and stiffness matrices defined by $[M] = [\Phi^g]^T[\mathbb{M}][\Phi]^g$, $[D] = [\Phi^g]^T[\mathbb{D}][\Phi]^g$ and $[K] = [\Phi^g]^T[\mathbb{K}][\Phi]^g$, where $\boldsymbol{f}(t) = [\Phi^g]^T \mathbb{F}(t)$ is the vector of the generalized forces and where $\boldsymbol{f}^{\mathrm{NL}}(\boldsymbol{q}^g(t), \dot{\boldsymbol{q}}^g(t)) = [\Phi^g]^T \mathbb{F}^{\mathrm{NL}}([\Phi]^g \boldsymbol{q}^g(t), [\Phi]^g \dot{\boldsymbol{q}}^g(t))$ is the vector of the generalized nonlinear forces. The dynamical systems we are interested in this paper are made up of few eigenvectors of global displacements. Consequently, the size of the nonlinear reduced-order computational model defined by Eqs. (6) to (8) is very small.

# 3   Application

In this Section, we present an industrial application of the methodology which consists in the dynamical analysis of a row of seven fuel assemblies with possibility of collisions between grids and submitted to a seismic loading.

## 3.1   Reference computational model

*(i)-Fuel assembly*

A fuel assembly is a slender structure which is made up of $264$ flexible fuel rods, $25$ stiff guide tubes and $10$ stiff grids which hold the tubes in position (see the finite element mesh in Fig. 1). The guide tubes are soldered to the grids while the fuel rods are fixed to the grids by springs. The longitudinal (vertical) direction is denoted by $\boldsymbol{z}$. The transverse directions are denoted by $\boldsymbol{x}$ and $\boldsymbol{y}$. The fuel rods and the guide tubes are
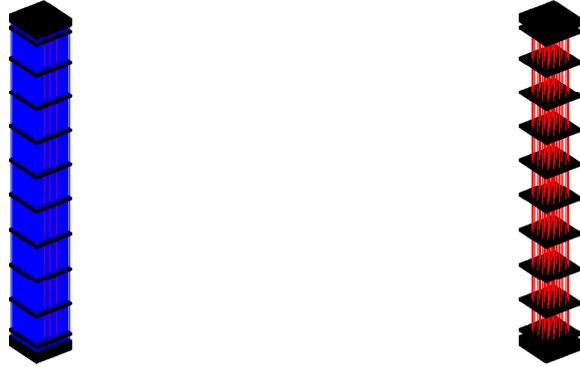


Figure 1: Finite element mesh of a fuel assembly: Grids (black), fuel rods (blue) and guide tubes (red). Left figure: Complete fuel assembly. Right figure: Grids and guide tubes only.

modeled by Timoshenko beams and the grids are modeled by solid elements. The end of guide tubes are fixed to the containment building. All the displacements following $\boldsymbol{y}$-direction are set to zero. For a single fuel assembly, the finite element model has $44,844$ elements and $449,580$ DOFs. There are $7,364$ elastic modes in the band $[0\,,400]$ Hz. The eight first elastic modes are ensemble modes (all the structure moves in phase), the corresponding eigenfrequencies are 3.09 Hz, 6.31 Hz, 9.78 Hz, 13.5 Hz, 17.6 Hz, 22.2 Hz, 27.3 Hz and 32.7 Hz. Beyond these ensemble modes, there are numerous local elastic modes (only a part of the structure moves) and a few global elastic modes (all the structure moves but not in phase). The 2nd elastic mode (global) and the 20th elastic mode (local) are plotted in Fig. 2.

*(ii)-Row of assemblies*

Concerning the linear part, the row of assemblies is made up of seven fuel assemblies. The fuel assemblies are linked each to the others by the rigid containment building on which an homogeneous seismic displacement is imposed. The gap between two assemblies is $2.09 \times 10^{-3}$ m. The gap between the leftmost assembly and the containment building $1.9 \times 10^{-3}$ m. The gap between the rightmost assembly and the containment
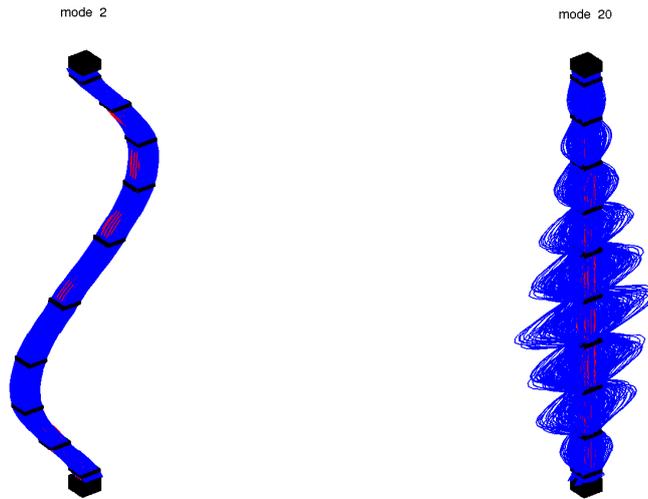
Figure 2: Left: $2^{\text{nd}}$ elastic mode (global). Rigth: $20^{\text{th}}$ elastic mode (local).

building $1.9 \times 10^{-3}$ m. The mesh of the finite element model is plotted in Fig. 3. The finite element model



Figure 3: Finite element mesh of a row of fuel assemblies: Grids (blue) and guide tubes (red). The fuel rods are not plotted.

has $313,908$ elements and $3,147,060$ DOFs and there are $51,548$ elastic modes in the band $[0,400]$ Hz (each mode of a single fuel assembly is reproduced seven times).

The possible contact grid/grid and grid/containment are taken into account by introducing $160$ elastic stops. Each grid has a left elastic stop and a right elastic stop, the containment building has $10$ elastic stops face to rightmost assembly grids and $10$ elastic stops face to leftmost assembly grids.

## 3.2 Construction and validation of the reduced-order computational model

In this section, a single fuel assembly is considered. The first step consists in the construction of the sub-domains $\Omega_j$ introduced in Section 2.2. Since we want to filter the local transverse displacements, the sub-domains are chosen as $100$ slides of equal thickness. The eigenvectors $\varphi_j^g$ are then computed following the

method introduced in Section 2.3. In the frequency band $[0\,,400]$ Hz, there are 35 eigenvectors. The $9^{\text{th}}$ eigenvector is plotted in Fig. 4. In the band $[0,400]$ Hz, the number of eigenvectors (35) is much lower than



Figure 4: $9^{\text{th}}$ eigenvector.

the number of elastic modes $(7,364)$. The accuracy of the reduced-order computational model should be analyzed by comparison with the reference computational model. However, the nonlinear transient response of the reference computational model is very difficult to calculate (the presence of localized nonlinearities requires the use of a very small time step for the integration scheme). Consequently, the accuracy analysis is carried out by comparing the linear frequency response functions of the reduced-order computational model without localized nonlinearities, with the frequency response functions of the reference computational model without localized nonlinearities. Nevertheless, a convergence analysis of the nonlinear responses with respect to the number of global eigenvectors will be carried out in Section 3.3. A Rayleigh damping model is used and is constructed for the frequencies 3 Hz and 400 Hz with a damping ratio $0.04$. A point load is applied to the node $P_{\text{exc}}$ which is located at the middle of the $9^{\text{th}}$ grid (from bottom to top). This load is equal to $1$ N in the frequency band $[0\,,400]$ Hz following $\boldsymbol{x}$-direction. The containment building is fixed. The measurement node $P_{\text{obs}}$ is located at the middle of the $4^{\text{th}}$ grid. The frequency response functions at points $P_{\text{obs}}$ and $P_{\text{exc}}$ are plotted in Figs. 5 and 6. These figures show a very good accuracy of the reduced-order



Figure 5: Modulus of the frequency response function of the acceleration in $\boldsymbol{x}$-direction at point $P_{\text{obs}}$: reduced-order computational model (solid line) and reference computational model (dashed line).
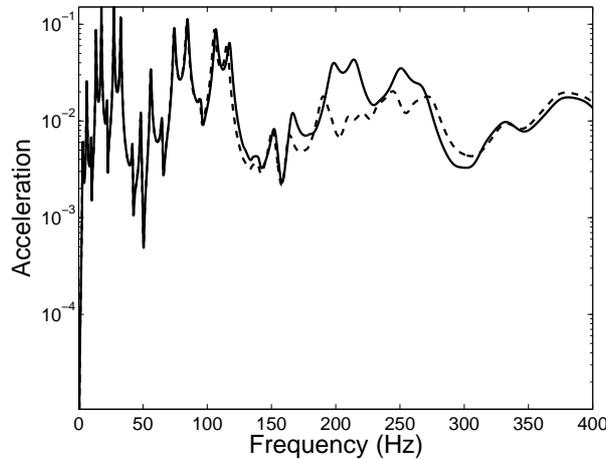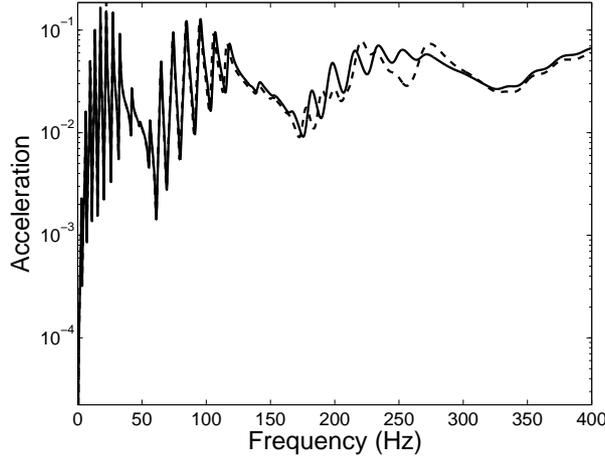
Figure 6: Modulus of the frequency response function of the acceleration in $x$-direction at point $P_{\text{exc}}$: reduced-order computational model (solid line) and reference computational model (dashed line).

computational model in the frequency band $[0\,,100]$ Hz. In the frequency band $[100\,,300]$ Hz, the accuracy of the reduced-order computational model is less. These small deviations are due to the local contributions in the neighborhood of the observation points, which are not taken into account when the basis of the global displacements space is used to construct the reduced-order computational model.

## 3.3   Nonlinear transient response of a row of fuel assemblies

Each fuel assembly of the row is decomposed into 100 slices yielding 700 subdomains. For the band $[0\,,400]$ Hz, the reduced-order computational model is constructed with 245 eigenvectors (instead of $51,548$ elastic modes which would be required with a classical modal analysis). The displacement of the containment building following $x$-direction is imposed and is denoted by $x_s(t)$. We are interested in the nonlinear transient relative displacement of the row of assemblies. The damping ratio is over $0.3$ for the seven first eigenmodes and the damping ratio is around $0.1$ for the other eigenmodes. The relative displacement vector is solution of Eqs. (6) to (8) with $\boldsymbol{f}(t) = -[\Phi^g]^T[\mathbb{M}][W]\ddot{x}_s(t)$ in which $[W]$ is a vector whose components are equal to 1 for all the DOFs corresponding to the displacements following $x$-direction and are equal to zero for the other DOFs. The function $t \mapsto \ddot{x}_s(t)$ is plotted in Figs. 7. The nonlinear relative response is
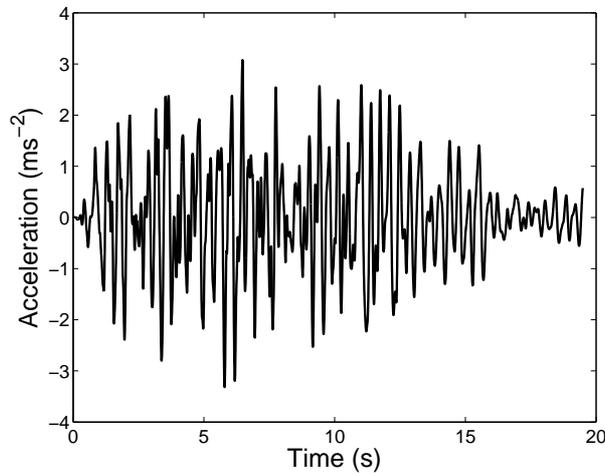


Figure 7: Function $t \mapsto \ddot{x}_s(t)$.

calculated in the interval time $[0\,,19.48]$ s using an explicit Euler integration scheme with an integration time step $10^{-5}$ s. The observation point $P_1$ belongs to the $1^{\text{st}}$ assembly (from left to right), and is located at the middle of $6^{\text{th}}$ grid (from bottom to top). For point $P_1$, the relative transient displacements is plotted in Fig. 8. The convergence of the contact forces between grids (nonlinear forces) with respect to the size of the global
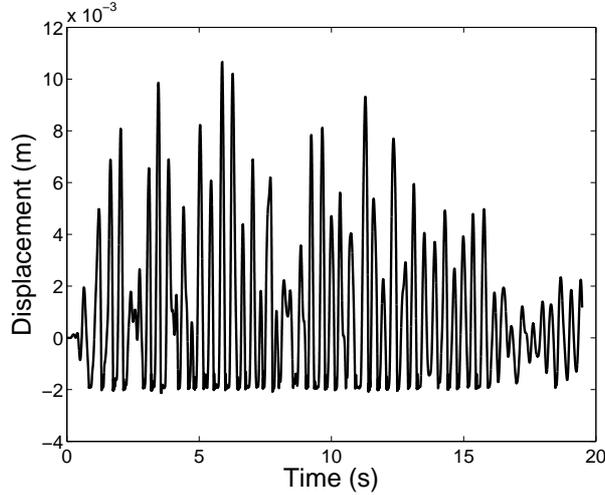


Figure 8: Relative transient displacement following $x$-direction for observation point $P_1$.

basis are analyzed for each elastic stop through the function $n_g \mapsto \int_0^T F_N(t;n_g)^2 dt$ in which $F_N(t,n_g)$ is the transient normal force calculated using $n_g$ global eigenvectors. The convergence function for point $P1$ is plotted on Fig. 9. From this figure, it can be seen that a good convergence of the nonlinear response is reached.
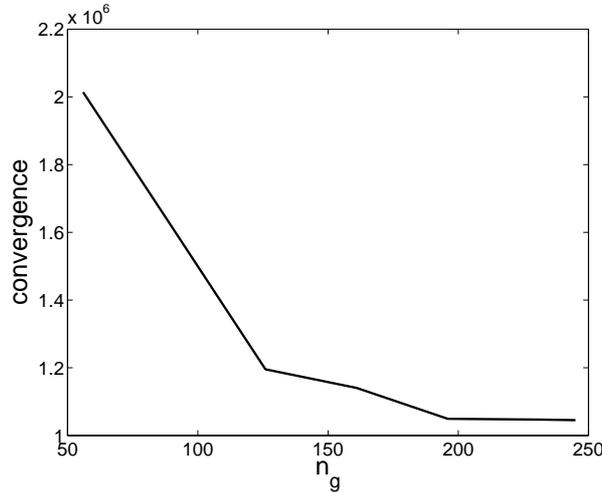


Figure 9: Convergence of the contact force for observation point $P_1$.

# 4  Conclusions

We have presented the construction a reduced-order computational model for nonlinear dynamical structures in presence of many local elastic modes in the low-frequency range. This method is based on the use of a

basis of the global displacements space. The constructed reduced-order computational model has a small dimension and allows the displacement of the stiff part of the structure to be predicted with a good accuracy. The methodology has successfully been applied to a complex industrial dynamical system for which the computational model has millions of degrees of freedom and numerous localized nonlinearities. The results show that the nonlinear dynamical response can be calculated with a good accuracy and a good convergence using only 245 eigenvectors.

# References

[1] K.J. Bathe, *Finite element Procedures*, Prentice Hall, 1996.

[2] T. Belytschko, W.L. Mindle, *Flexural Wave-propagation Behavior of Lumped Mass Approximations*, Computer and Structures 12(6) (1980) 805-812.

[3] H.C. Chan, C.W. Cai, Y.K. Cheung, *Convergence Studies of Dynamic Analysis by Using the Finite Element Method with Lumped Mass Matrix*, Journal of Sound and Vibration 165(2) (1993), 193-207.

[4] R.R. Craig, A.J. Kurdila, *Fundmentals of Structural Dynamics*, 2nd Edition, John Wiley and Sons, New Jersey, 2006.

[5] R.J. Guyan, *Reduction of Stiffness and Mass Matrices*, AIAA Journal 3 (1965) 380-388.

[6] J.L. Guyader, *Modal sampling method for the vibration study of systems of high modal density*, J. Acoust. Soc. Am. 88(5) (1990) 2269-2270.

[7] M.S. Jensen, *High Convergence Order Finite Elements With Lumped Mass Matrix*, International Journal for Numerical Methods in Engineering 39(11) (1996) 1879-1888.

[8] L. Ji, B.R. Mace, Pinnington R., *A mode-based approach for the mid-frequency vibration analysis of coupled long- and short-wavelength structures*. Journal of Sound and Vibration 289(1) (2006) 148-1700.

[9] K. Karhunen, *Zur Spektraltheorie Stochasticher Prozesse*, Ann. Acad. Sci. Fennicae 220 (1945).

[10] R.S. Langley, P. Bremmer, *A Hybrid Method for the Vibration Analysis of Complex Structural-Acoustic Systems*, J. Acoust. Soc. Am. 105(3) (1999) 1657-1672.

[11] M. Loève, *Probability Theory*, 3rd ed., Van Nostrand, New York, 1963.

[12] A.K. Noor, M.S. Anderson, W.H. Greene, *Continuum Models for Beam- and Platelike-Lattice Structures*, AIAA Journal 16(12) (1978) 1219-1228.

[13] J. Planchard, *Vibration of nuclear fuel assemblies: a simplified model*, Nuclear Engineering and Design 86(3) (1995) 383-391.

[14] C. Soize, A. Batou, *Stochastic reduced-order model in low-frequency dynamics in presence of numerous local elastic modes*, Journal of Applied Mechanics - Transactions of the ASME 78(6) (2011) 061003.